Cell Stem Cell
Article

Erythropoietin Preserves the Endothelial Differentiation Capacity of Cardiac Progenitor Cells and Reduces Heart Failure during Anticancer Therapies

Melanie Hoch,[1,8] Philipp Fischer,[1,8] Britta Stapel,[1] Ewa Missol-Kolka,[1] Belaid Sekkali,[5] Michaela Scherr,[2] Fabrice Favret,[6] Thomas Braun,[7] Matthias Eder,[2] Karin Schuster-Gossler,[3] Achim Gossler,[3] Andres Hilfiker,[4] Jean-Luc Balligand,[5] Helmut Drexler,[1] and Denise Hilfiker-Kleiner[1,*]
[1]Department of Cardiology and Angiology
[2]Department of Haematology, Haemostasis, Oncology, and Stem Cell Transplantation
[3]Department of Molecular Biology
[4]Department of HTTG
Medical School Hannover, 30625 Hannover, Germany
[5]University of Louvain Medical School, Experimental and Clinical Research Institute, 1200 Brussels, Belgium
[6]Université Paris 13, EA 2363 "Réponses cellulaires et fonctionnelles à l'hypoxie," 93017 Paris, France
[7]Max-Planck-Institute for Heart and Lung Research, 61231 Bad Nauheim, Germany
[8]These authors contributed equally to this work
*Correspondence: hilfiker.denise@mh-hannover.de
DOI 10.1016/j.stem.2011.07.001

SUMMARY

Anticancer therapies, such as targeting of STAT3 or the use of anthracyclins (doxorubicin), can induce cardiomyopathy. In mice prone to developing heart failure as a result of reduced cardiac STAT3 expression (cardiomyocyte-restricted deficiency of STAT3) or treatment with doxorubicin, we observed impaired endothelial differentiation capacity of Sca-1$^+$ cardiac progenitor cells (CPCs) in conjunction with attenuated CCL2/CCR2 activation. Mice in both models also displayed reduced erythropoietin (EPO) levels in the cardiac microenvironment. EPO binds to CPCs and seems to be responsible for maintaining an active CCL2/CCR2 system. Supplementation with the EPO derivative CERA in a hematocrit-inactive low dose was sufficient to upregulate CCL2, restore endothelial differentiation of CPCs, and preserve the cardiac microvasculature and cardiac function in both mouse models. Thus, low-dose EPO treatment could potentially be exploited as a therapeutic strategy to reduce the risk of heart failure in certain treatment regimens.

INTRODUCTION

Recent studies indicate that the heart exhibits intrinsic regenerative capacity during disease and aging, which may attenuate the progression of heart failure (Hsieh et al., 2007). Activation and differentiation of resident cardiac progenitor cells have been implicated in healing processes in response to acute or chronic myocardial damage (Oh et al., 2003; Torella et al., 2004). However, only a few intracellular pathways have well-characterized roles in cardiac progenitor cell proliferation and differentiation (see Table S1 available online; Madonna et al., 2009; Mohri et al., 2009; Zelarayán et al., 2008; Iwakura et al., 2011). Likewise, little is known about regulatory factors in the cardiac microenvironment.

The anthracyclin doxorubicin (DOX) has been used effectively to treat a broad range of cancers. The clinical usage and efficacy of DOX is, however, restricted by the side effects observed, most notably heart failure (Ferreira et al., 2008). Similarly, blocking STAT3 signaling via antisense RNA interference (RNAi), peptides, or small molecular inhibitors can lead to successful suppression of tumor cell growth and apoptosis, making STAT3 an attractive molecular target for the development of novel cancer therapeutics (Deng et al., 2007). However, it has also been shown previously that downregulation of STAT3 predisposes the heart to failure (Hilfiker-Kleiner et al., 2004, 2007; Jacoby et al., 2003). Here we analyzed whether the endogenous cardiac regeneration potential of resident Sca-1-positive cardiac progenitor cells (CPCs) is impaired in failure-prone hearts of mice with a cardiomyocyte-specific knockout of STAT3 (α*MHC-Cre*$^{tg/+}$; *STAT3*$^{flox/flox}$, CKO) or in mice exposed to treatment with DOX.

We observed that in both heart failure models, CPCs display severely impaired endothelial differentiation capacity that is related to a reduced activation state of the CCL2/CCR2 system in the CPCs. We also found that CKO- and DOX-treated mice display alterations in the cardiac microenvironment that include a depletion of cardiac erythropoietin (EPO) and discovered a positive interaction between paracrine EPO and the autocrine CCL2/CCR2 system in CPCs. Overall, our results suggest that treatment with synthetic EPO derivatives could preserve the endothelial differentiation potential of CPCs during certain anticancer treatment programs.

RESULTS

Sca-1$^+$ Cardiac Progenitor Cells Express CCR2 and EPOR but Are Devoid of FLK-1

Freshly isolated Sca-1$^+$ cardiac progenitor cells (CPCs) from hearts of 3-month-old wild-type mice expressed Nanog and

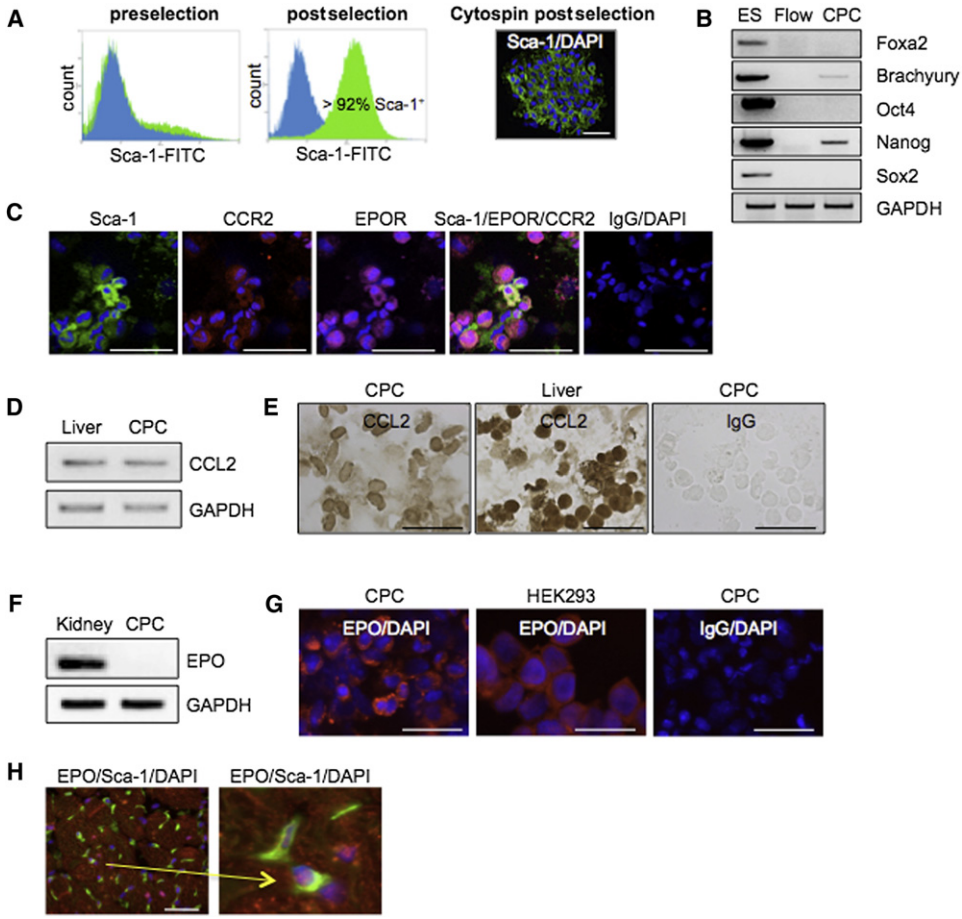

Figure 1. Isolation and Characterization of WT-CPCs

(A) FACS analyses of myocardial cells before and after MACS selection for Sca-1 (left and middle; Sca-1$^+$ cardiac cells, green; IgG control, blue). Cytospin of Sca-1$^+$ CPCs followed by Sca-1 immunohistochemistry (IHC) (right: Sca-1, green; nuclear stain with DAPI, blue). Scale bar represents 50 μm.

(B) RT-PCR for Foxa2, Brachyury, Oct4, Nanog, and Sox2 in freshly isolated CPCs and Sca-1 negative flow through (Flow) in comparison with mouse embryonic stem cells (ESCs). GAPDH served as control for equal cDNA content.

(C) Confocal microscopy displayed CPCs positive for Sca-1 (green, left), CCR2 (red, second from left), EPOR (purple, middle), DAPI (blue), and merged (second from right). Isotype control (IgGs for CCR2 and EPOR, right). Scale bars represent 50 μm.

(D) RT-PCR displayed abundance of CCL2 mRNA in liver cells and in freshly isolated WT-CPCs. Loading control used was GAPDH.

(E) Cytospin followed by CCL2 IHC in freshly isolated WT-CPCs (left), liver cells (middle), and isotype control for CCL2 (right). Scale bars represent 50 μm.

(F) EPO mRNA was below detection level by RT-PCR (40 cycles) in freshly isolated WT-CPCs; mouse kidney served as positive control; loading control was GAPDH.

(G) Cytospin followed by IHC displayed EPO-positive cells (EPO, red; nuclear stain DAPI, blue) among WT-CPCs (left), human embryonic kidney cells (HEK293, middle) served as positive control, isotype control for EPO (IgG, right). Scale bars represent 50 μm.

(H) IHC showed small cells double positive for EPO (red, DAPI, blue) and Sca-1 (green) in adult WT LVs, right panel displayed larger magnification of area pointed out by the arrow in the left panel. Scale bar represents 50 μm.

All data were confirmed in at least three independent CPC isolations derived from pooled hearts of 8 to 20 adult male mice. See also Figure S1.

Brachyury but showed no expression of Oct4, Sox2, or Foxa2 (Figures 1A and 1B). The expression of surface markers typically present on hematopoietic or endothelial progenitor cells, CD45, CD34, CD133, and CD117 (c-kit), or endothelial markers like FLK-1, VE-Cadherin (CD144), and VCAM-1 (CD106) were not detected, while about 25% of CPCs expressed CD105, 30% CD31, 45% CD13, 60% CD73, 28% CD90, 13% CD29, 17% CD44, 28% the chemokine (C-C motif) receptor-2 (CCR2), and 29% the erythropoietin receptor (EPOR) (Figure S1). The majority of CPCs expressing CCR2 were also positive for EPOR (Figure 1C). Freshly isolated CPCs expressed mRNA and protein of the CCR2 ligand CCL2 (Figures 1D and 1E); EPO mRNA was not detectable despite positive staining for EPO protein (Figures 1F and 1G). Immunohistology of heart sections revealed EPO/Sca-1 double-positive small cells located between cardiomyocytes (Figure 1H), suggesting that CPCs bind to EPO protein present in the cardiac microenvironment.

CPCs Differentiate into Endothelial Cells, Adipocytes, Fibroblasts, and Pericytes

For in vitro differentiation, CPCs were cultivated for 4 weeks on fibronectin-coated plates where they formed a closed cell layer

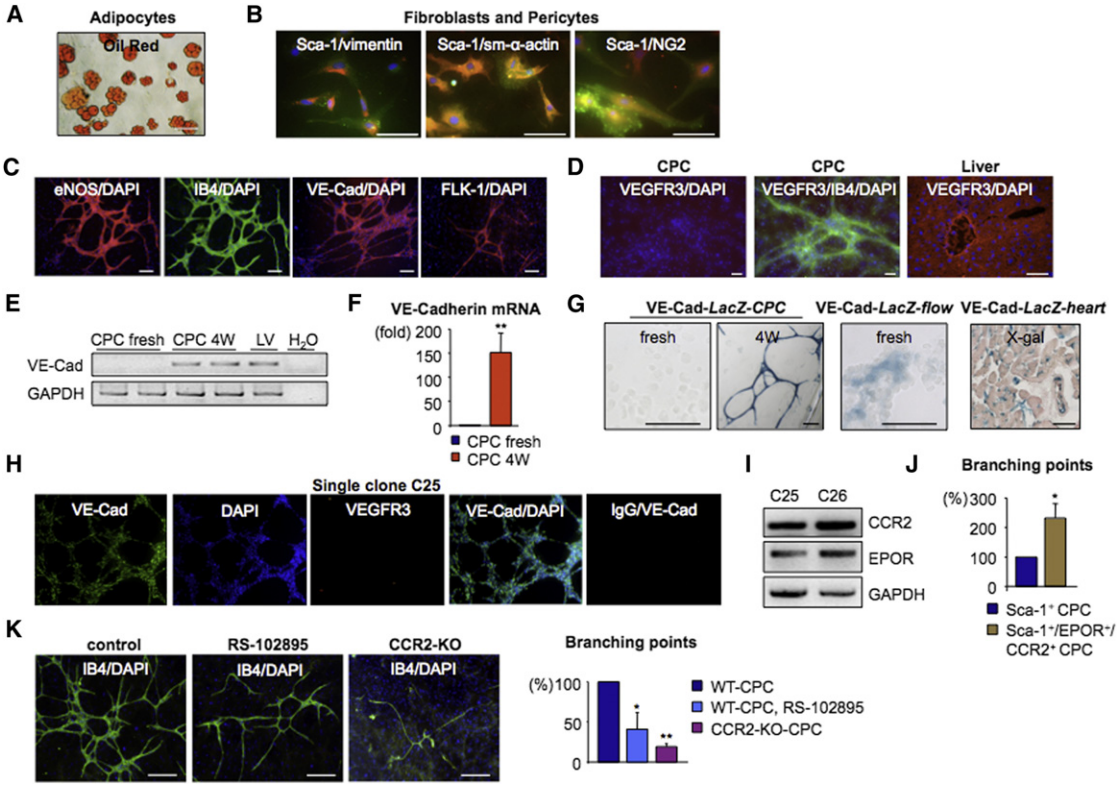

Figure 2. Differentiation Potential of CPCs

(A and B) CPCs differentiated into (A) adipocytes (oil red) and (B) fibroblasts/pericytes (Sca-1, green; vimentin, sm-α-actin, and NG2, red) during in vitro cultivation. Scale bars represent 50 μm.

(C) Endothelial nets differentiated from WT-CPCs stained positive for eNOS (red, left), IB4 (green, second from left), VE-Cadherin (red, second from right), FLK-1 (red, right), and DAPI (blue). Scale bars represent 100 μm.

(D) Endothelial nets differentiated from WT-CPCs (IB4, green, middle) are negative for VEGFR3 (red, left), DAPI (blue). Positive control for VEGFR3 staining: liver (right). Scale bars represent 100 μm.

(E and F) Bar graph (F) summarizing VE-Cadherin mRNA levels (qRT-PCR) and agarose gels showing VE-Cadherin mRNA amplified by RT-PCR (E) in freshly isolated CPCs, in CPCs after 4 weeks (4W) of in vitro cultivation (LV served as positive control for VE-Cadherin PCR, GAPDH was used to control for equal cDNA content).

(G) LacZ staining (blue) of CPCs isolated from *VE-Cadherin-Cre*$^{tg/+}$; ROSA26R mice stained immediately after isolation (left) and after 4 weeks of in vitro cultivation (second from left). The parallel flow through of Sca-1-negative cells (second from right) and LV sections (right) from *VE-Cadherin-Cre*$^{tg/+}$; ROSA26R mice served as positive control for VE-Cadherin-Cre induction. Scale bars represent 50 μm.

(H) Endothelial nets on matrigel derived from a CPC clone (C25, Table S2) stained for VE-Cadherin (green, left), DAPI (blue, second from left), and VEGFR3 (red, middle), merged (green/blue, second from right). IgG served as control for specificity of VE-Cadherin staining (right).

(I) RT-PCR revealed expression of CCR2 and EPOR mRNA in expanded single clones C25 and C26 (Table S2), Loading control: GAPDH.

(J) The bar graph summarizes branching points of endothelial nets from sorted Sca-1$^+$ CPCs and Sca-1$^+$/EPOR$^+$/CCR2$^+$ CPCs (*$p < 0.05$, Sca-1$^+$ CPCs were set to 100%).

(K) Endothelial net formation (IB4, green; DAPI, blue) of CPCs alone (left) or with the CCR2 blocker RS-102895 (100 nM, middle) or of CCR2-KO-CPCs (right). The bar graph summarizes number of branching points (WT-CPCs = 100% in each parallel cell isolation, *$p < 0.05$, **$p < 0.01$ versus untreated WT-CPCs, scale bars represent 200 μm).

All data summarize at least three independent CPC isolations derived from pooled hearts of 8 to 20 adult male mice. Error bars indicate SD. See also Figure S2.

containing adipocytes, fibroblasts, pericytes (Figures 2A and 2B), and endothelial cells (Figure 2C). Endothelial cells stained positive for VE-Cadherin, FLK-1, eNOS, and isolectin B4 (IB4) but were negative for VEGFR3 (Figures 2C and 2D), indicating that they displayed a vascular endothelial phenotype (Tammela et al., 2008). Endothelial differentiation of CPCs during in vitro cultivation was evident by upregulation of VE-Cadherin and FLK-1 mRNA (Figures 2E and 2F; Figure S2). To monitor endothelial differentiation, we used *VE-Cadherin-Cre*$^{tg/+}$; ROSA26R mice in which endothelial cells are marked by *lacZ* expression (Benedito et al., 2009). Freshly isolated *VE-Cadherin-Cre*$^{tg/+}$; ROSA26R CPCs were initially negative for LacZ staining but give rise to LacZ-positive endothelial cell nets during in vitro cultivation (Figure 2G). Endothelial differentiation of CPCs was also confirmed in CPC clones expanded from single cells. Five successfully expanded CPC clones maintained an undifferentiated phenotype during expansion as indicated by expression of Sca-1 and Nanog but not VE-Cadherin (Table S2). Cultivation of clones on matrigel was used to stimulate endothelial differentiation. Two of the five clones underwent vasculogenic

Table 1. Cardiac Function in WT and CKO Mice with CERA or Saline

	WT Baseline	WT Saline	WT CERA	CKO Baseline	CKO Saline	CKO CERA
%FS	33 ± 7	31 ± 8	32 ± 7	29 ± 10	22 ± 9[a]	34 ± 5[b]
LVEDD	4.7 ± 1.0	4.1 ± 0.4	4.2 ± 0.3	4.3 ± 0.5	4.3 ± 0.6	4.1 ± 0.4
LVESD	3.4 ± 0.8	2.8 ± 0.5	3.0 ± 0.5	3.1 ± 0.8	3.3 ± 0.7	2.7 ± 0.4
HR	444 ± 22	448 ± 61	472 ± 35	435 ± 25	477 ± 56	481 ± 54

LV end-diastolic (LVEDD, mm) and end-systolic diameter (LVESD, mm), fractional shortening (%FS), and heart rate (HR, beats/min) determined by echocardiography.
n = 4 to 10 mice per measurement.
[a] $p < 0.05$ versus WT baseline.
[b] $p < 0.05$ CKO CERA versus CKO saline.

endothelial differentiation on matrigel, as confirmed by positive staining for VE-Cadherin and negative staining for VEGFR3 (Figure 2H). Both clones expressed EPOR and CCR2 (Figure 2I), suggesting that subpopulations that are double positive for EPOR and CCR2 harbor endothelial differentiation potential. Enrichment for EPOR/CCR2 double-positive CPCs by FACS sorting led to higher endothelial differentiation on fibronectin-coated plates (Figure 2J; VE-Cadherin qRT-PCR, +303% ± 117%, $p < 0.05$ versus Sca-1-sorted CPCs) compared to Sca-1-sorted CPCs. Depletion of CD31 did not affect the endothelial differentiation of CPCs (Figure S2), but blocking CCR2 with RS-102895 did have an inhibitory effect (Figure 2K; VE-Cadherin qRT-PCR: −47% ± 8%, $p < 0.05$ versus WT-CPCs). Consistently, CPCs isolated from *CCR2*$^{-/-}$ knockout mice (CCR2-KO-CPCs) also displayed impaired endothelial differentiation (Figure 2K).

Impaired Endothelial Differentiation of CPCs in Mice with a Cardiomyocyte-Specific Deletion for STAT3 Is Associated with Reduced CCL2/CCR2 Activation

Male mice with a cardiomyocyte-specific STAT3 deletion (CKO) are prone to develop heart failure with aging (Hilfiker-Kleiner et al., 2004). CPCs isolated from young CKO males (CKO-CPCs) without obvious signs of heart failure (Table 1) displayed impaired endothelial differentiation compared to CPCs (WT-CPCs) isolated from corresponding wild-type littermates (WT: *STAT3*$^{flox/flox}$) (Figures 3A and 3B). The impaired endothelial differentiation of CKO-CPCs was not associated with STAT3 deletion in the CPCs when freshly isolated or after 4 weeks of in vitro cultivation (Figures 3C and 3D), consistent with the fact that no α*MHC-Cre*$^{tg/+}$ transgene activity could be observed in CPCs isolated from α*MHC-Cre*$^{tg/+}$; ROSA26R mice (less than 0.001% CPCs stained positive for LacZ; Figure S3). FACS analyses showed that the expression of CCR2 was markedly lower on CKO-CPCs compared to WT-CPCs while the expression of EPOR was unchanged (Figure 3E). FACS and qRT-PCR analyses showed no differences in the expression of CD31, CD105, CD73, CD13, and CD144 (data not shown) between CKO-CPCs and WT-CPCs, suggesting that there is no major difference in CPC subpopulations between the two genotypes.

qRT-PCR revealed no difference in the expression of CCL2 between freshly isolated CKO-CPCs and WT-CPCs (data not shown). It is known, however, that endogenous CCR2 blockers can be generated by MMP-12-mediated proteolytic cleavage of CCL2 into a CCL2 subfragment that then acts as a CCR2 antagonist (Dean et al., 2008). MMP-12 mRNA levels were upregulated in CKO hearts (qRT-PCR: CKO: +1479% ± 328%, $p < 0.01$ versus WT) and in CKO-CPCs (qRT-PCR: CKO-CPCs 4W in vitro cultivation +453% ± 98%, $p < 0.01$ versus WT-CPCs; freshly isolated CKO-CPCs +225% ± 203%, $p < 0.05$ versus WT-CPCs). Combined addition of the MMP-12 blocker PF-356231 and recombinant CCL2 (rCCL2) to CKO-CPCs increased the endothelial differentiation of CKO-CPCs whereas addition of rCCL2 alone had no significant effect (Figure 3F). Conversely, addition of recombinant MMP-12 to WT-CPCs impaired their endothelial differentiation (Figure 3G). Whole tissue extracts from CKO hearts displayed enhanced cleavage of rCCL2 into the antagonistic CCL2 subfragment compared to WT tissue extracts, which could be attenuated by the MMP-12 inhibitor PF-356231 (Figure 3H).

Erythropoietin Expression Is Reduced in CKO Hearts

Because we observed that CPCs bind EPO protein within the cardiac microenvironment, we analyzed EPO expression in CKO hearts. CKO mice displayed a marked reduction in cardiac EPO protein levels compared to corresponding WT mice (Figures 4A and 4B; Figure S5), which was associated with reduced EPO mRNA levels (9-fold lower determined by microarray analysis from five pooled CKO versus five pooled WT LVs, data not shown). Like cardiomyocytes in the adult mouse heart, isolated neonatal rat cardiomyocytes (NRCM) expressed and secreted EPO into the cell culture supernatant (0.013 to 0.402 ng/ml supernatant per 10^6 seeded cardiomyocytes) (Figures 4C–4E). EPO in NRCM supernatant was able to induce erythropoiesis in a methylcellulose-CFU-assay with freshly isolated murine bone marrow cells (BMC). The erythropoiesis capacity of NRCM supernatant was lost after heat inactivation (Figure 4E) or if supernatant derived from NRCM where EPO had been downregulated by siRNA (Figure 4F). Knockdown of STAT3 using a shRNA-lentivirus in NRCM resulted in a 2-fold reduction of EPO protein levels compared to NRCM infected with a control lentivirus (Figure 4D), suggesting that EPO expression in NRCM depends in part on STAT3.

Treatment of CKO Mice with the EPO Derivative CERA Upregulates CCL2 and Restores Endothelial Differentiation of CKO-CPCs but Has No Effect in CPCs from CCR2 Knockout Mice

To investigate whether exogenous supplementation of the CKO myocardium with EPO could restore endothelial differentiation of CKO-CPCs in vivo, a 3 week treatment with the EPO derivative CERA (continuous erythropoiesis receptor activator, that is

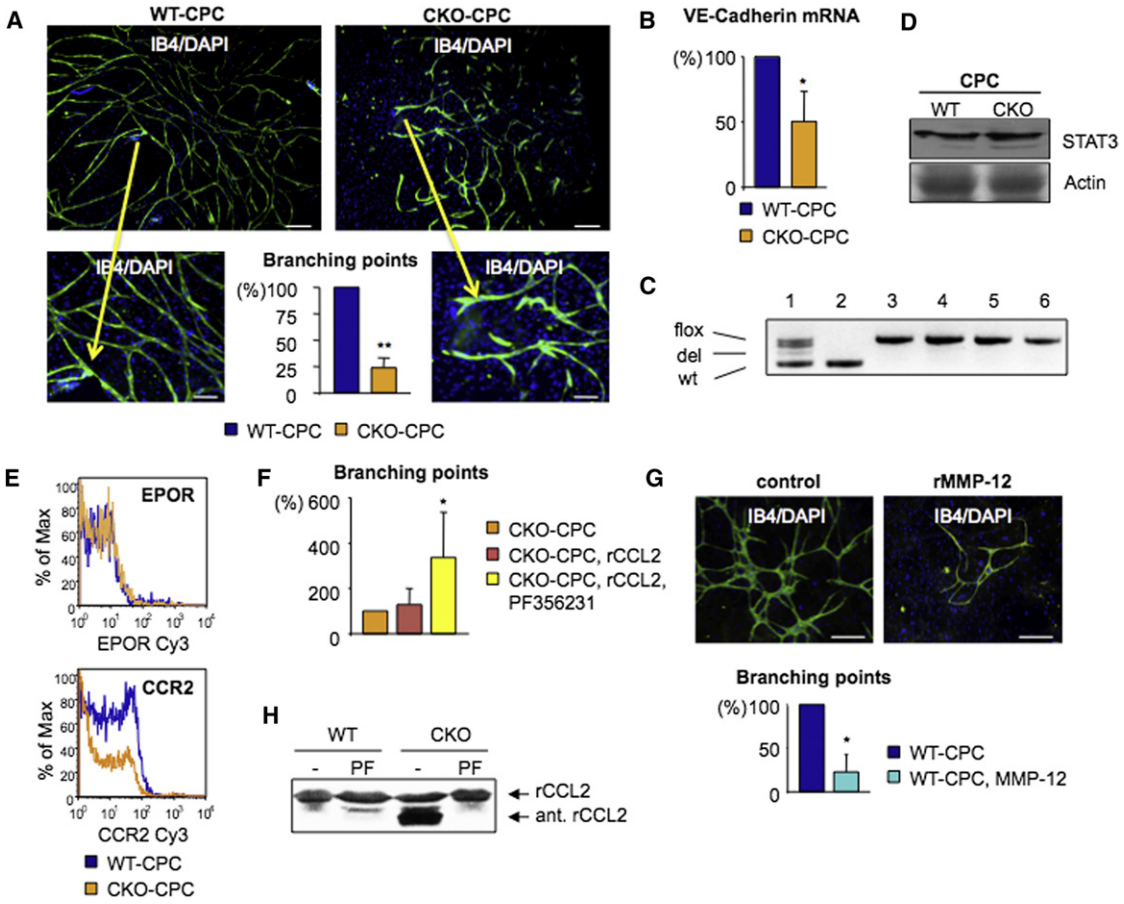

Figure 3. CKO-CPCs Displayed Impaired Endothelial Net Formation as a Potential Consequence of Modulated CCR2 Activity

(A and B) Impaired endothelial net formation (IB4, green; DAPI, blue) of CKO-CPCs (right) compared to WT-CPCs (left), scale bars in upper panels represent 200 μm and in lower panels represent 100 μm, the bar graph summarizes number of branching points (WT-CPCs = 100% in each set, $^{**}p < 0.01$) (A) and qRT-PCR for VE-Cadherin in WT-CPCs and CKO-CPCs after 4 weeks of cultivation (WT-CPCs = 100%, $^{*}p < 0.05$) (B).

(C) Agarose gel depicting PCR-based detection of wild-type STAT3, floxed STAT3, and flox-deleted STAT3 alleles in genomic DNA from a heterozygous *Cre*$^{tg/+}$; *STAT3*$^{flox/+}$ (1) and a wild-type mouse heart (2), from freshly isolated WT-CPCs (*STAT3*$^{flox/flox}$) (3) and CKO-CPCs (*Cre*$^{tg/+}$; *STAT3*$^{flox/flox}$) (4), and from WT-CPCs (*STAT3*$^{flox/flox}$) (5) or CKO-CPCs (*Cre*$^{tg/+}$; *STAT3*$^{flox/flox}$) after 4 weeks in culture (6).

(D) Representative western blot displayed similar levels of STAT3 protein in WT-CPCs and CKO-CPCs after 4 weeks of culture; loading control was actin.

(E) Quantification of EPOR (top) and CCR2 (bottom) in freshly isolated CKO-CPCs and WT-CPCs by FACS.

(F) Bar graph summarizes number of branching points in CKO-CPC cultures alone (set at 100%), with addition of rCCL2 or with addition of rCCL2 and PF-356231 ($^{*}p < 0.05$ versus untreated CKO-CPCs).

(G) Endothelial net formation (IB4, green; DAPI, blue) of WT-CPCs alone (left) and with addition of rMMP-12 (200 ng/ml; right). The bar graph summarizes number of branching points (WT-CPCs = 100% in each parallel cell isolation, $^{*}p < 0.05$, versus untreated WT-CPCs). Scale bars represent 200 μm.

(H) Western blot depicted CCL2 forms generated from recombinant CCL2 (rCCL2: 3.6 μg/ml LV extract), antagonistic rCCL2 (ant. rCCL2) by WT and CKO heart extracts ex vivo with or without addition of the MMP-12 inhibitor PF-356231 (30 nM).

All results derive from three to seven independent cell isolations pooled from 8 to 20 adult male mice. Error bars indicate SD. See also Figure S3.

methoxy polyethylene glycol-epoetin beta from Roche) at a low dose that did not increase the hematocrit (3 μg/kg/week; Figure S4) was used. Low-dose CERA had no influence on the recruitment of BMC to the myocardium as indicated by similar numbers of X-gal-positive cells in wild-type mice transplanted with bone marrow from ROSA26 mice expressing the bacterial *lacZ* gene (Figure S4). In freshly isolated CKO-CPCs from CERA-treated mice, CCL2 mRNA levels were markedly higher and MMP-12 mRNA levels were lower compared to CKO-CPCs from placebo-treated CKO mice (Figure 4G). Endothelial differentiation of CKO-CPCs was substantially higher in CERA compared to placebo-treated CKO mice after in vitro cultivation (Figure 4H; VE-Cadherin qRT-PCR: CKO-CPCs/CERA, +157% ± 5%, $p < 0.05$ versus CKO-CPC/placebo). Expression of Delta-like 4 (Dll4) a marker for sprouting activity of endothelial cells (Nakagami et al., 2006) was readily detectable in sprouting ends of endothelial nets formed by WT-CPCs or CKO-CPCs from CERA-treated CKO mice but was only marginal in CKO-CPCs from placebo-treated CKO mice (Figure 4I). CERA treatment had no additional effect on endothelial differentiation of WT-CPCs (Figure 4H). In contrast to CKO-CPCs, CERA treatment of CCR2-KO mice did not improve endothelial differentiation of CCR2-KO-CPCs (qRT-PCR for VE-Cadherin: +5% ± 8% with CERA, n.s. versus CCR2-KO-CPCs/saline).

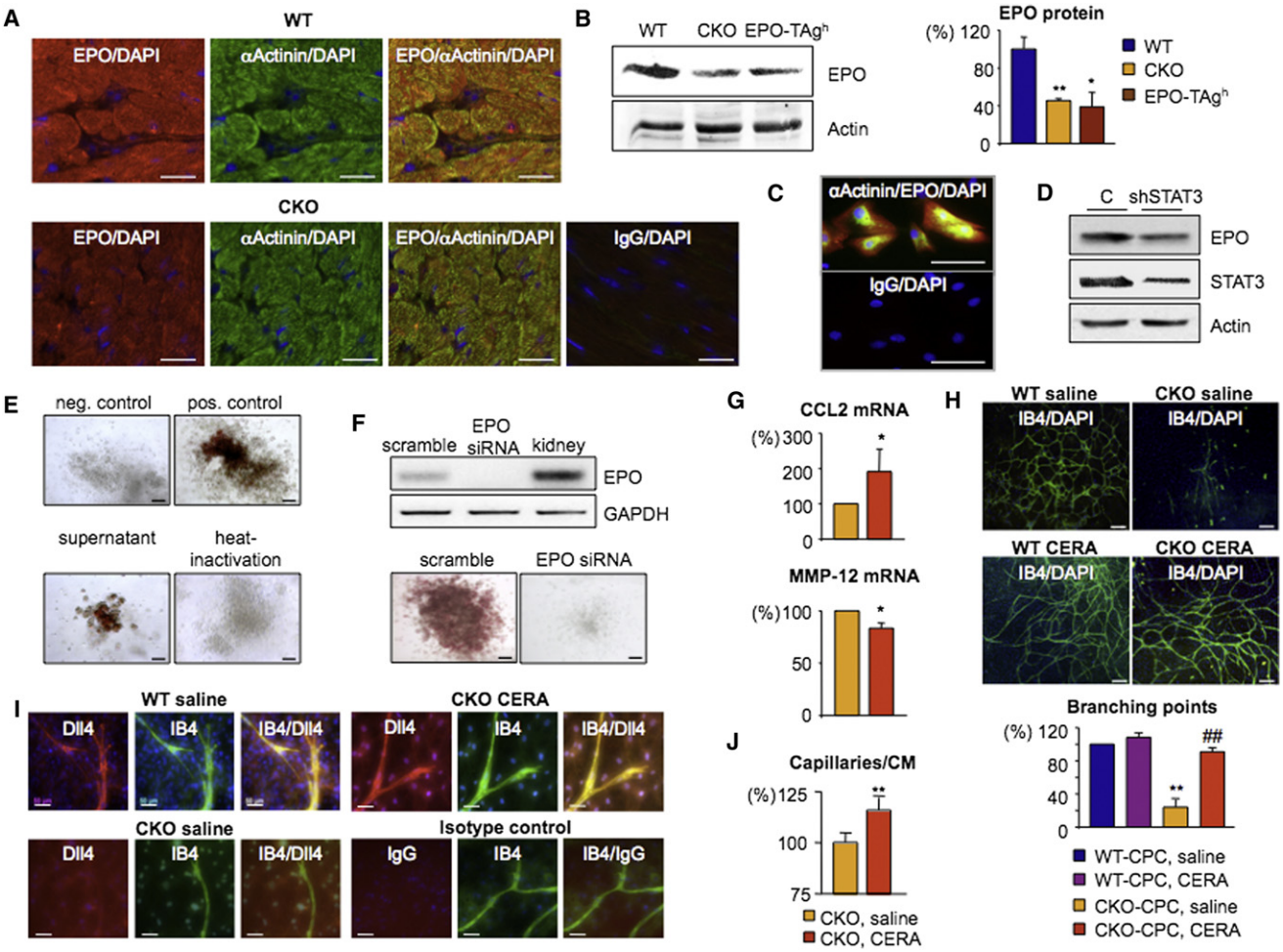

Figure 4. Endogenous EPO Is Reduced in CKO Mice; Supplementation with the EPO-Derivative CERA Exerts Positive Effects on CPCs and the Cardiac Phenotype of CKO Mice

(A) Representative IHC showed EPO (red) located in cardiomyocytes (positive for α-sarcomeric actinin; α-actinin, green) in WT (top) and CKO (bottom) LV sections, overlay of EPO/α-actinin: red/green, DAPI (blue), isotype control for EPO (IgG/DAPI). Scale bars represent 25 μm.

(B) Western blot depicted EPO protein levels in LVs from WT, CKO, and EPO-TAg^h mice. Loading control was actin. The bar graph summarizes EPO protein levels, *$p < 0.05$, **$p < 0.01$ versus WT.

(C) IHC visualizing EPO protein (green, double-stained with anti-α-actinin red, nuclear stain with DAPI, blue; top) in cultured neonatal rat cardiomyocytes (NRCM), isotype control for EPO (IgG, DAPI; bottom).

(D) Western blot depicted EPO protein levels in NRCM transduced with control lentivirus (C) or shSTAT3-RNA lentivirus (shSTAT3). Loading control was actin.

(E) Outgrowth of erythroid colony- and burst-forming units (CFU-/BFU-E) from freshly isolated mouse BMC in methylcellulose assays with no addition of rEPO (negative control; bottom left), supplemented with rEPO (positive control; top right) or cell culture supernatant from NRCM, native or heat inactivated (lower left and right).

(F) qRT-PCR for EPO expression in NRCM treated with scrambled or EPO siRNA. Outgrowth of erythroid CFU-/BFU-E from freshly isolated mouse BMC in methylcellulose assays with cell culture supernatant from NRCM treated with scrambled siRNA (left) or EPO siRNA (right).

(G) Bar graphs depicting CCL2 and MMP-12 mRNA levels (qRT-PCR) in freshly isolated CKO-CPCs from saline or CERA-treated CKO mice (saline-treated mice were set at 100%, *$p < 0.05$).

(H) Endothelial net formation (IB4, green) of WT-CPCs or CKO-CPCs isolated from saline or CERA-treated WT and CKO mice, number of branching points were summarized in the bar graph (WT-CPCs = 100% in each isolation, **$p < 0.01$ versus WT-CPCs saline, ##$p < 0.01$ CKO-CPCs with CERA versus CKO-CPCs control). Scale bars represent 200 μm.

(I) Sprouting ends of endothelial nets stained with antibodies against Delta-like 4 (Dll4, red), IB4 (green), and DAPI (blue), and isotype control for Dll4. Scale bars represent 50 μm.

(J) The capillary to cardiomyocytes ratio summarized in the bar graph from LV sections of CKO mice treated with saline or CERA (**$p < 0.01$ versus saline-treated CKO).

All results derive from four to six mice per group and from three independent cell isolations pooled from six to ten mice. Error bars indicate SD. See also Figures S4 and S5.

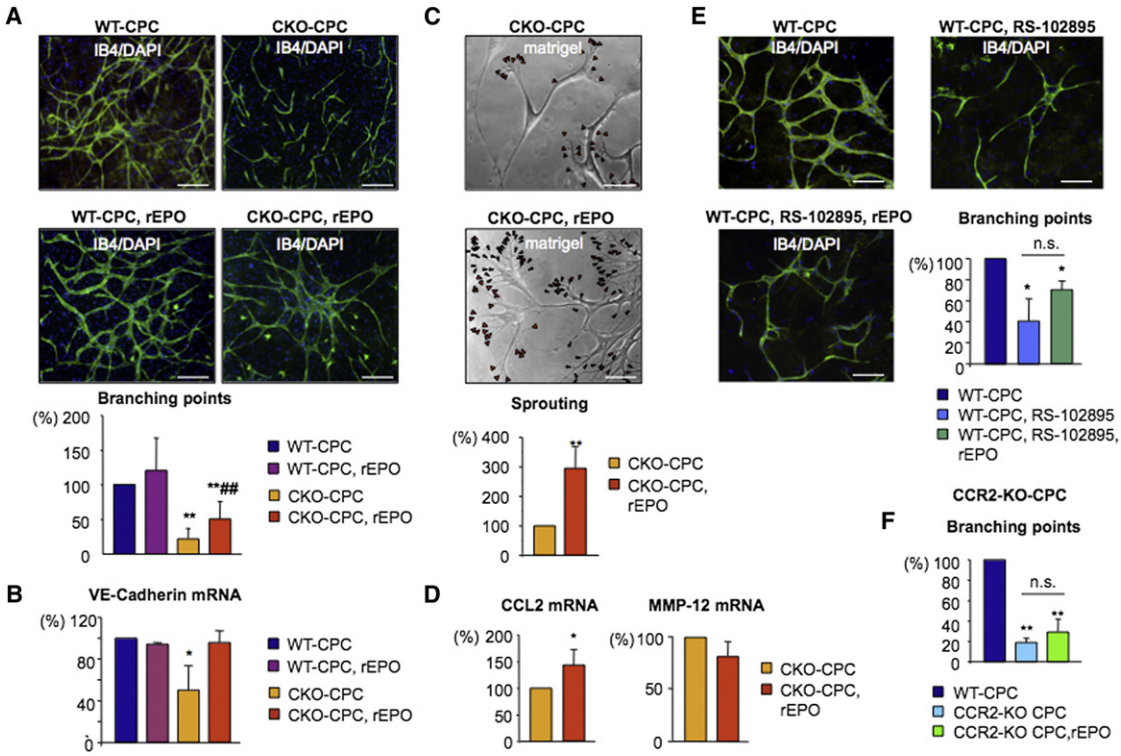

Figure 5. Recombinant EPO Improved Endothelial Net Formation and Increased CCL2 Expression in CKO-CPC Cultures but Had No Effect on CCR2-KO-CPCs

(A) Endothelial nets (IB4, green) in WT-CPC (left) or CKO-CPC (right) cultures with or without addition of rEPO (1.2 U/ml). Scale bars represent 200 μm. The bar graph summarizes number of branching points of endothelial nets (nontreated WT-CPC cultures were set at 100%, **$p < 0.01$ versus nontreated WT-CPCs; ##$p < 0.01$ rEPO treated versus nontreated CKO-CPCs).

(B) Bar graph summarizing VE-Cadherin mRNA levels (qRT-PCR) in WT-CPCs and CKO-CPCs cultured with or without rEPO (*$p < 0.05$ versus nontreated WT-CPCs).

(C) Sprouting ability of CKO-CPCs on matrigel with (bottom) or without addition of rEPO (top), number of branching points were summarized in the bar graph; **$p < 0.01$ versus nontreated CKO-CPCs. Scale bars represent 50 μm.

(D) The bar graphs summarize CCL2 and MMP-12 mRNA levels (qRT-PCR) in CKO-CPC cultures with or without addition of rEPO (nontreated CKO-CPC cultures = 100%, *$p < 0.05$).

(E) Endothelial nets (IB4, green) in parallel cultures of WT-CPCs (set 100%; top left) with RS-102895 (top right) or with RS-102895 and rEPO (bottom left) (number of branching points were summarized in the bar graph, *$p < 0.05$, versus WT-CPC cultures). Scale bars represent 100 μm.

(F) Bar graph summarizing number of branching points in parallel cultures of WT-CPCs and CCR2-KO-CPCs (**$p < 0.01$, versus WT-CPC cultures).

Results in all experiments derive from three to seven cell isolations each from pools of eight to ten mouse hearts. Error bars indicate SD. See also Figure S5.

CERA Prevents Onset of Heart Failure and Preserves Capillary Density without Altering the Inflammatory Status in CKO Mice

In line with previous data (Hilfiker-Kleiner et al., 2004), placebo-treated CKO mice displayed a diminishment of capillaries, a decrease in LV function (Table 1), and an increase in atrial natriuretic peptide (ANP) mRNA expression (ANP qRT-PCR: CKO placebo: +691% ± 453%, $p < 0.05$ versus placebo-treated WT) compared to placebo-treated WT mice. CERA treatment prevented the reduction in capillary density (Figure 4J), the decrease in LV function (Table 1), and the increase in ANP mRNA expression (CKO CERA: +136% ± 204%, n.s. versus placebo-treated WT). CERA treatment did not alter the number of CD45-positive inflammatory cells, mainly macrophages and leukocytes, in CKO hearts (Figure S4). In contrast to CKO hearts, CERA had no effect on the myocardial capillary density (capillaries/cardiomyocytes in WT placebo: 1.61 ± 0.1 versus WT CERA: 1.58 ± 0.06, n.s.), the cardiac function (Table 1), or the ANP expression (WT CERA: −7% ± 82%, n.s. versus WT placebo) in WT mice.

Addition of Recombinant EPO Improves Endothelial Differentiation of CKO-CPCs In Vitro but Has No Effect on WT-CPCs with Blocked CCR2 or on CCR2-KO-CPCs

To analyze whether EPO directly improved the endothelial differentiation of CKO-CPCs, recombinant mouse EPO (rEPO) was added to CKO-CPCs during in vitro cultivation. Figures 5A and 5B show that rEPO significantly improved endothelial differentiation of CKO-CPCs but did not affect that of WT-CPCs. In contrast to rEPO, rVEGF could not improve endothelial differentiation of CKO-CPCs (Figure S5). Addition of rEPO increased also the sprouting ability of CKO-CPCs on matrigel (Figure 5C) and markedly increased CCL2 expression in CKO-CPCs, but had no effect on MMP-12 expression (Figure 5D). A luciferase reporter plasmid harboring the putative CCL2 promoter

(nucleotides –3043 to −21, relative to the transcription start of CCL2) showed that rEPO augmented CCL2 promoter activity (Figure S5).

In contrast to CKO-CPCs, rEPO was not able to improve impaired endothelial differentiation in WT-CPCs treated with the CCR2 blocker RS-102895 (Figure 5E, confirmed by qRT-PCR for VE-Cadherin: rEPO/RS-102895: −68% ± 10% versus RS-102895: −47% ± 15%, n.s.). Similarly, rEPO could not rescue the impaired endothelial differentiation seen in CCR2-KO-CPCs (Figure 5F).

Doxorubicin Treatment Decreases CCL2 Expression and Impairs Endothelial Differentiation of CPCs and Lowers Cardiac EPO Protein Levels

We analyzed the CPC phenotype in a second model of progressive heart failure based on doxorubicin-induced cardiomyopathy (DOX: 6 mg/kg/week for 3 weeks) in wild-type mice (8-week-old male Balb/C mice). CPCs isolated from DOX-treated mice (DOX-CPCs) displayed impaired endothelial differentiation (Figures 6A and 6B) and reduced CCL2 expression (Figure 6C) compared to CPCs from placebo (saline)-treated control mice, whereas MMP-12 expression was not affected (Figure 6C). DOX treatment reduced cardiac EPO protein levels (Figure 6D). Addition of DOX to NRCM markedly lowered their STAT3 and EPO expression (Figure 6E).

CERA Preserves CCL2 Expression and Endothelial Differentiation in CPCs, Maintains Cardiac Capillary Density and Cardiac Function, and Improves Survival of Doxorubicin-Treated Mice

Low-dose CERA (3 μg/kg/week) starting 1 day before DOX treatment prevented impairment of endothelial differentiation (Figures 6A and 6B, qRT-PCR for VE-Cadherin: DOX-CPCs/CERA: +75% ± 45%, $p < 0.05$ versus DOX-CPCs/placebo) and preserved CCL2 expression in DOX-CPCs (Figure 6C). As observed by others (Kunisada et al., 2000), DOX reduced cardiac capillary density, induced heart failure, and caused a high mortality rate in mice; all of these features were markedly attenuated by cotreatment with CERA (Figures 6F–6H).

EPO Protein Expression Is Reduced in End-Stage Failing Human Hearts

We previously described a group of patients with end-stage heart failure resulting from dilatative cardiomyopathy (DCM) or ischemic cardiomyopathy (ICM) that displayed a substantial reduction of STAT3 protein levels in LV tissue compared to non-failing hearts (NF) (Podewski et al., 2003). We found that in LV tissue samples of the same hearts, EPO protein levels were reduced (Figure S6), highlighting a parallel between our findings in mouse and human hearts with cardiomyopathy.

DISCUSSION

We present evidence that subpopulations of CPCs can differentiate in endothelial cells, adipocytes, and fibroblasts/pericytes. As observed by others (Oh et al., 2003), CPCs express the typical surface markers CD45, CD34, CD117 (c-kit), CD133, and FLK-1 that are present on bone-marrow-derived progenitor cells at a very low level if at all, suggesting that they constitute a distinct population of residential progenitor cells within the heart. Clonal expansion of CPCs revealed stable expression patterns of Sca-1 and Nanog but no expression of VE-Cadherin. Under endothelial differentiation conditions on matrigel, CPC clones expressing CCR2 and EPOR were able to differentiate in VE-Cadherin-positive, VEGFR3-negative (Tammela et al., 2008) vasculogenic endothelial cells, a property confirmed in CPCs carrying the endothelial VE-Cadherin reporter system. Some CPCs exhibit a mesenchymal progenitor cell-like phenotype as indicated by the surface markers CD13, CD73, CD29, CD44, and CD90 (Pittenger and Martin, 2004) and differentiation into cell types of the mesenchymal lineage, i.e., adipocytes, fibroblasts, and pericytes, indicating that CPCs consist of a heterogeneous population of progenitor cells with distinct differentiation potentials.

The CCL2/CCR2 system is important for neoangiogenesis during tissue regeneration, as shown by the fact that CCR2-KO mice display delayed neoangiogenesis in injured skeletal muscle (Contreras-Shannon et al., 2007). We confirmed previously described (Salcedo et al., 2000) direct proangiogenic signaling via the CCR2 on endothelial cells and expand the angiogenic role of CCR2 from mature endothelial cells to endothelial differentiation of CPCs, as CPCs lacking CCR2 function through deletion or pharmacological block display substantially lower endothelial differentiation capacities. It is important to note that with these assays we cannot distinguish whether the CCL2/CCR2 system primarily promotes endothelial differentiation from CPCs and/or promotes branching of endothelial cells differentiated from CPCs.

We detected an attenuated CCL2/CCR2 system associated with impaired endothelial differentiation in CPCs isolated from failure-prone hearts of CKO mice (Hilfiker-Kleiner et al., 2004) and in failing hearts from WT mice exposed to DOX. Impairment of the CCL2/CCR2 system in CKO-CPCs results from alterations in the cardiac microenvironment caused by the STAT3 deficiency in cardiomyocytes and includes reduced expression of CCR2 and impaired autocrine CCL2 signaling due to enhanced generation of antagonistic CCL2 fragments. We do not have evidence for a shift in Sca-1$^+$ subpopulations because other surface markers were not different relative to WT-CPCs. Increased MMP-12 expression in CKO-CPCs and CKO hearts was responsible for the proteolytic cleavage of CCL2 in its antagonistic fragment. We speculate that the resulting CCR2 antagonism may result in a negative feedback mechanism that could explain the downregulation of CCR2 on CKO-CPCs. We have no explanation why the expression of MMP-12 is upregulated in cardiac tissue of CKO mice and in isolated CKO-CPCs. However, we conclude that the upregulation of MMP-12 and the subsequent generation of antagonistic CCL2 plays a crucial role for impaired endothelial differentiation of CKO-CPCs, because (1) enhanced MMP-12-mediated CCL2 cleavage was observed in CKO hearts, a finding that is consistent with previous reports showing that MMP-12 cleaves CCL2, -7, -8, and -13 in CCR antagonists (Dean et al., 2008); (2) inhibition of MMP-12 activity and addition of rCCL2 improved endothelial differentiation of CKO-CPCs, whereas addition of rCCL2 alone had no effect; (3) addition of rMMP-12 to WT-CPCs impaired their endothelial differentiation; and (4) improved endothelial differentiation of

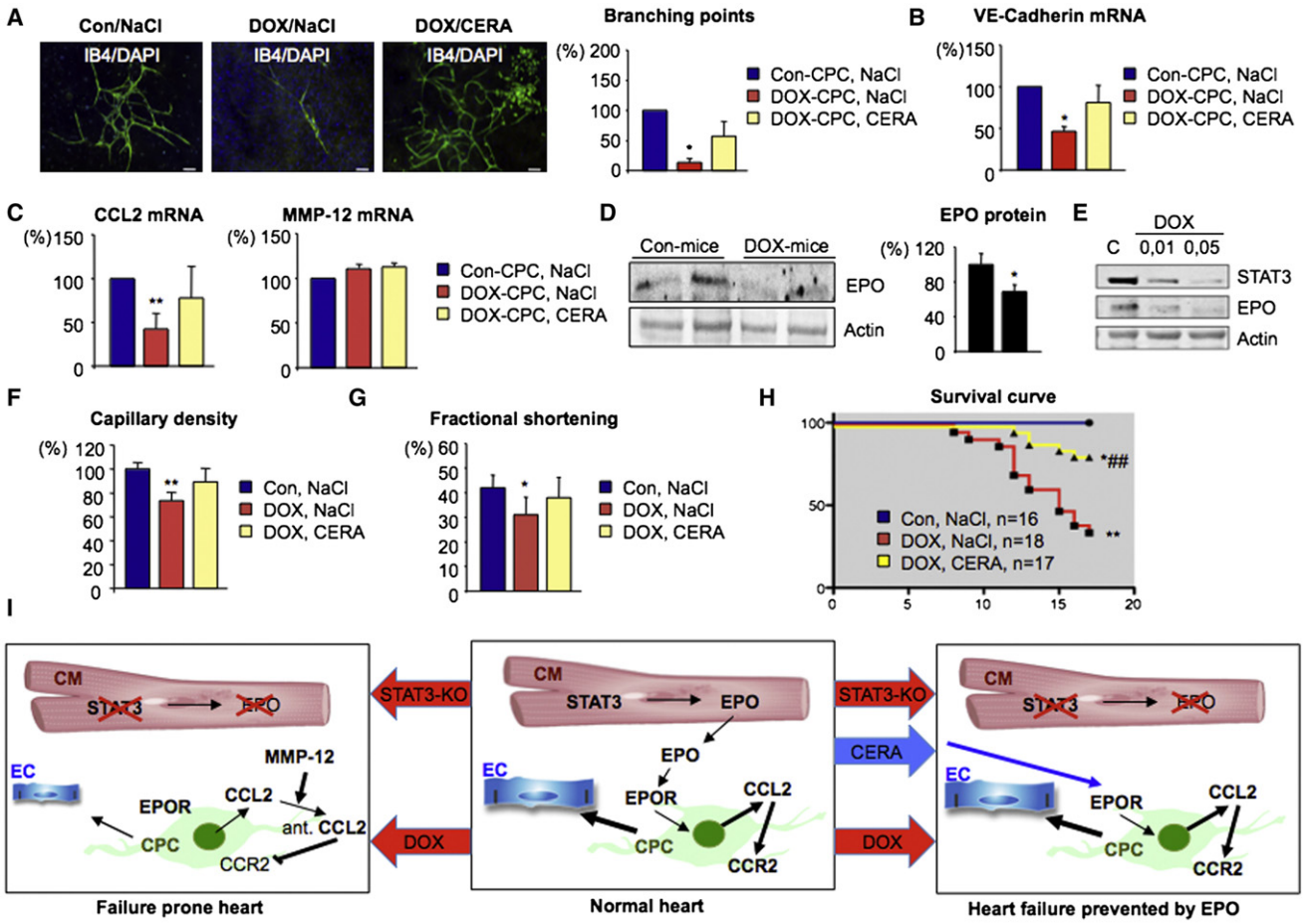

Figure 6. Negative Effect of Doxorubicin on Cardiac EPO Expression, CPC Phenotype, Capillary Density, Cardiac Function, and Survival Was Attenuated by CERA

(A) Endothelial net formation (IB4, green) of CPCs isolated from saline control (Con: set at 100% in parallel cultures; left) and of DOX-CPCs in vivo treated with or without CERA (right and middle) followed by 4 weeks in vitro cultivation. The bar graph summarizes number of branching points (Con-CPCs = 100% in each isolation). Scale bars represent 50 μm.

(B) The bar graph shows VE-Cadherin mRNA (qRT-PCR) levels of Con-CPCs (set at 100% in parallel cultures; *$p < 0.05$ versus Con-CPCs) and DOX-CPCs after in vivo treatment with or without CERA followed by 4 weeks in vitro cultivation.

(C) Bar graphs summarizing qRT-PCR for CCL2 and MMP-12 mRNA levels in freshly isolated Con-CPCs (set at 100% in parallel cultures) and DOX-CPCs after in vivo treatment with or without CERA, **$p < 0.01$ versus Con-CPCs.

(D) Western blot depicting EPO protein levels in Con and DOX mice, the bar graph summarizes EPO protein levels, *$p < 0.05$ versus Con mice.

(E) Western blot depicting EPO and STAT3 protein levels in NRCM treated with DOX; loading control, Actin.

(F–H) The bar graph summarizes ratios of capillaries/cardiomyocytes (F), the fractional shortening (%FS) determined by echocardiography (G), and the Kaplan Meier survival curve in Con mice or DOX mice treated with saline or CERA (H) (*$p < 0.05$, **$p < 0.01$ versus WT mice/saline; **$p < 0.01$ #DOX mice/CERA versus DOX mice/saline).

All results (A–H) derive from 5–18 mice per group and 3 independent cell isolations (pools of 6–10 mice).

(I) Scheme explaining how cardiac STAT3 deficiency or DOX may impair the endogenous cardiac vasculogenic regeneration potential. Middle: In the normal heart, STAT3-dependent paracrine factors possibly including EPO are secreted from cardiomyocytes (CM) into the cardiac microenvironment to maintain the endothelial differentiation capacity of CPCs into endothelial cells (EC) a characteristic that involves the autocrine CCL2/CCR2 system on CPCs. Left: Cardiac STAT3 deficiency (STAT3-KO) alters the cardiac microenvironment, i.e., diminishes EPO protein levels and impairs the CCL2/CCR2 system on CPCs by reducing CCR2 and by promoting MMP-12 expression. MMP-12 generates cleaved antagonistic CCL2 (ant. CCL2). As a result, CCR2 signaling is hampered and endothelial differentiation of CPCs is reduced. DOX affects the cardiac microenvironment in a similar way (in part also via reducing STAT3) as evidenced by decreased EPO levels. In addition, DOX reduces CCL2 expression of CPCs and thereby reduces CCR2 activity, leading to attenuated endothelial differentiation of CPCs. This impaired endothelial differentiation of CPCs in STAT3 deficiency and DOX treatment diminishes the cardiac vasculature and contributes to heart failure. Right: In treatment regimens using DOX or STAT3 reduction, low-dose CERA supplementation increases the activation state of the CCL2/CCR2 system in the heart and specifically in CPCs thereby protecting vascular cells and potentially also the cardiomyocyte compartment.

Error bars indicate SD. See also Figure S6.

CKO-CPCs isolated from CERA-treated CKO mice was associated with upregulated CCL2 and reduced expression of MMP-12.

In DOX-CPCs, CCR2 and MMP-12 expression were normal, but CCL2 expression was markedly reduced. As EPO directly increases CCL2 promoter activity, the reduced CCL2 expression

in DOX-CPCs may be at least in part a consequence of lower EPO levels in the cardiac microenvironment of DOX-treated mice. In fact, DOX reduced EPO expression in cardiomyocytes in vitro. Furthermore, CPCs bind EPO in the cardiac microenvironment since EPO protein was detected on freshly isolated CPCs without evidence that these cells expressed EPO mRNA themselves.

Upregulation of endogenous cardiac EPO signaling has been described during ischemic insults (Lin et al., 2008; Tada et al., 2006) and in pressure overload-induced LV dysfunction (Asaumi et al., 2007). We observed low levels of endogenous cardiac EPO in adult mouse and human hearts that seem to be derived at least in part from cardiomyocytes that express and secrete EPO under normoxic conditions. Cardiomyocyte STAT3 appears important for this basal cardiac EPO expression as EPO protein levels were lower in CKO mice, in end-stage failing human myocardium with reduced STAT3 expression (Podewski et al., 2003) and in isolated cardiomyocytes with shRNA-mediated STAT3 knockdown. Consistent with our data, a 4-fold downregulation of EPO expression in hearts from patients with nonischemic heart failure has been described via microarray analysis (E-GEOD-1869) (Kittleson et al., 2005). Moreover, it has been reported that DOX reduces myocardial STAT3 expression (Kunisada et al., 2000), a feature that we confirmed in isolated cardiomyocytes. In line with a proposed role for STAT3 in cardiac EPO expression, we observed that hearts and cultured cardiomyocytes exposed to DOX treatment displayed reduced EPO protein levels. We do not know at this point precisely how the lower endogenous EPO protein level in hearts from CKO and DOX mice affects their cardiac phenotype. However, we found that treatment of CKO-CPCs with rEPO in vitro or treatment of CKO mice and DOX mice in vivo with the EPO derivative CERA upregulated CCL2 expression and improved endothelial differentiation, apparently mainly via the CCL2/CCR2 system, because rEPO (in vitro) or CERA (in vivo) could not improve endothelial differentiation of CCR2-KO-CPCs. rEPO was also not able to rescue impaired endothelial differentiation in WT-CPCs with pharmacologically blocked CCR2. Previous studies have shown that non-hematocrit-inducing EPO derivatives can also directly protect cardiomyocytes from apoptosis (Ueba et al., 2010). EPO treatment also induced CCL2 promoter activity in cardiomyocytes and, because CCL2 can protect cardiomyocytes from apoptosis (Tarzami et al., 2005) and promote regeneration of cardiomyocytes by inducing migration of neuronal crest cells into the injured heart (Tamura et al., 2011), the link between EPO and CCL2 signaling may be beneficial not only for the cardiac vasculature but also for other cardiac cells. The cardioprotective effect seen with CERA treatment in the two mouse models that we studied could therefore be multifaceted. It is also consistent with recently published data indicating that low-dose hematocrit-inactive or nonerythropoietic synthetic EPO-mimicking compounds exert protective effects in cardiomyopathies (Vogiatzi et al., 2010; Bergmann et al., 2011). In contrast, however, hematocrit-increasing high doses of EPO seem to be problematic in the treatment of cardiomyopathies, especially myocardial infarction (Najjar et al., 2011).

Our finding that EPO did not further enhance endothelial differentiation in wild-type CPCs and that CERA had no specific proangiogenic effect in normal hearts suggests that it is not inducing supranormal angiogenesis, which might be an important aspect with regard to a potential use of EPO derivatives for cardioprotection (and possibly also protection of other organs) during antitumor strategies involving DOX treatment or STAT3 inhibition. Importantly, there is already evidence that EPO does not promote tumor growth during DOX treatment (Chen et al., 2007; Gewirtz et al., 2006). This activity profile contrasts positively with other cardioprotective proangiogenic factors, such as VEGF, that clearly promote tumor angiogenesis and therefore could not be used to protect the heart during anticancer therapies.

In conclusion, our report highlights the importance of the CCL2/CCR2 system for sustaining the endogenous vasculogenic regeneration potential of CPCs and potentially also endothelial cells in a VEGF-independent manner in the adult heart. In failure-prone situations induced by cardiotoxic antitumor therapies with DOX or STAT3 deficiency, the CCL2/CCR2 system is disrupted due to impaired autocrine mechanisms in CPCs and impaired paracrine systems possibly involving cardiomyocyte-derived EPO. However, treatment with rEPO or the EPO-derivative CERA preserved the endothelial differentiation of CPCs in CKO and DOX mice by upregulating CCL2 and preserved cardiac vasculature and function in vivo. Therefore, EPO administration at low, hematocrit-inactive, doses seems an attractive avenue to pursue for protecting the heart during antineoplastic drug therapy and might also have broader applications in cardiac regeneration.

EXPERIMENTAL PROCEDURES

Recombinant human fibroblast growth factor (rhFGF-basic, R&D systems), cell culture medium (DMEM/F12 1:1), HBSS, and PBS were from GIBCO, Invitrogen. All other chemicals were from SIGMA-ALDERICH.

Patient Data

LV tissues were from patients undergoing heart transplantation due to end-stage heart failure caused by dilatative (DCM, n = 4) or ischemic (ICM, n = 2) cardiomyopathy. LV tissue from donor hearts not suited for transplantation served as control (NF, n = 6).

Animal Experiments

3-month-old male mice with a cardiomyocyte-restricted knockout of STAT3 (CKO: $\alpha MHC\text{-}Cre^{tg/+}$; $STAT3^{flox/flox}$) and wild-type (WT: $STAT3^{flox/flox}$) mice were used as described previously (Hilfiker-Kleiner et al., 2004). Crossing $\alpha MHC\text{-}Cre^{tg/+}$ mice to $ROSA^{flox/flox}$ mice generated $\alpha MHC\text{-}Cre^{tg/+}$; ROSA26R mice. The tamoxifen-inducible VE-Cadherin-Cre mice were crossed with $ROSA^{flox/flox}$ to generate $VE\text{-}Cadherin\text{-}Cre^{tg/+}$; ROSA26R reporter mice and induced as described (Benedito et al., 2009). Generation of EPO-TAg^{h} mice for experimental controls is described (El Hasnaoui-Saadani et al., 2009). $CCR2^{-/-}$ and ROSA26R mice were purchased from the Jackson Laboratory. C57Bl/6 and Balb/C mice were from Charles River.

Mice were injected weekly (i.p.) with CERA dissolved in saline (3 μg/kgBW Mircera, Roche) or with saline for 3 subsequent weeks. Balb/c mice (8 weeks old) were injected weekly (i.p.) with doxorubicin hydrochloride (DOX) dissolved in saline (6 mg/kgBW DOX/week, SIGMA) or with saline or CERA (3 μg/kgBW Mircera, Roche) for 3 subsequent weeks. Echocardiography was performed in sedated mice (isoflurane inhalation 0.5%) using a Vevo 770 (Visual Sonics) as described (Hilfiker-Kleiner et al., 2007).

All animal studies were in compliance with the Guide for the Care and Use of Laboratory Animals as published by the U.S. National Institutes of Health and were approved by our local Institutional Review Boards.

Isolation, Characterization, and Cultivation of Sca-1^{+} Cardiac Progenitor Cells

The Sca-1-FITC microbead kit with the Magnetic Cell Sorting (MACS) system (Miltenyi Biotec) was used for isolation of Sca-1^{+} cells from mouse hearts

(Oh et al., 2003; Supplemental Experimental Procedures). The protocol for clonal expansion of CPCs is given in the Supplemental Information. Purity and marker profile of freshly isolated CPCs was determined by FACS analysis (FACS Calibur and LSRII, BD Biosciences) with antibodies against Sca-1, CD31, CD34, CD45, CD144, CD106, CD13, CD29, CD44, CD73, CD90 (BD PharMingen), CD4, CD105, c-kit (CD117), prominin-1 (CD133) (Miltenyi Biotech), CD144 (eBioscience), CCR2 (Abcam), EPOR, and FLK-1 (Santa Cruz Biotechnology). In most experiments, MACS-isolated CPCs were used. Only where specifically indicated, CPCs were subsequently sorted by FACS (MoFlow, XPD Upgrade, Beckman-Coulter) for EPOR (Santa Cruz Biotechnology) and CCR2 (Abcam) and seeded on fibronectin-coated wells. Mouse rEPO (1.2 U/ml, R&D Systems), mouse rMMP-12 (200 ng/ml, R&D Systems), mouse rVEGF (100 ng/ml; SIGMA), the CCR2-inhibitor RS-102895 (100 nM, SIGMA), rCCL2 (100 ng/ml; Immunotols), or the MMP12-inhibitor PF-356231 (30 nM, Enzo Life Science) were added to CPCs cultures 24 hr after seeding and replaced every 3rd day. Controls were supplemented with the same volume of PBS or DMSO.

Isolation and Transduction of Neonatal Rat Cardiomyocytes

Isolation and cultivation of neonatal rat cardiomyocytes (NRCM) were described previously (Hilfiker-Kleiner et al., 2004). Generation of anti-c-STAT3-small-hairpin-RNAs (shRNA) corresponding to position 823 to 841 of the murine c-STAT3 gene (Genbank accession number NM-213659), lentiviral transgene plasmids pdc-SR, and shRNA was described previously (Haghikia et al., 2010). Scrambled siRNA or EPO siRNA (Santa Cruz Biotechnology) were transfected into NRCM by Lipofectamin 2000 (Invitrogen). NRCM were treated for 24 hr with DOX (0.01 and 0.05 μg/ml).

Colony-Forming Cell Assays for Mouse Cells

Freshly isolated BMCs (tibia and femur) from C57Bl/6 mice (2×10^4 cells per 35 mm dish) were used to analyze the colony-forming activity in semisolid methylcellulose (Methocult GF M3534, StemCell technologies) according to the manufacturer's protocol with slight modifications (Miller and Lai, 2005) supplemented with rEPO (3 U/ml, positive control) or concentrated NRCM-supernatants (10×), cells were analyzed with an Axiovert 200M with Axiovision 4.6 software (Carl Zeiss).

Matrigel Tube Formation Assay

Matrigel tube formation assay was performed as described by Tepper et al. (2002). In brief, a 48-well plate was precoated with 100 μl Matrigel (GFR basement membrane matrigel matrix, BD Biosciences). CPCs were seeded at a density of 1.25×10^4 cells per well in DMEM/F12 (1:1) with 2% FBS and 1.2 U/ml rEPO. Control medium was supplemented with the same volume of PBS. The number of sprouts per cell was determined.

Immunohistochemistry

For immunohistochemistry, CPCs (cytospins and cultures), and NRCM were fixed with 4% paraformaldehyde (PFA). LV cryosections were fixed with ice-cold acetone as described (Hilfiker-Kleiner et al., 2004). After air-drying and rehydration in 1× PBS, the protocols from vectastain were used with the following antibodies: eNOS (Dianova), CD144 (VE-Cadherin) (Bender Medsystems), CD45, CD144, Ly-6G+C, VEGFR3 (BD PharMingen), αActinin, sm-α-actin (SIGMA), vimentin (Dako), NG2 (Millipore), CCR2, Dll4 (Abcam), Moma-2 (Acris), CCL2, EPO, EPOR, and FLK-1 (Santa Cruz Biotechnology) or with IB4 (Vector). For nuclear staining DAPI, Hoechst 33258 (SIGMA) or hematoxyline was used. Images were taken by fluorescence microscopy with Axiovision 4.6 software (Carl Zeiss, Jena, Germany) or by confocal laser microscopy (Leica DM IRB with TCS SP2 AOBS scan head). X-gal staining is depicted in the Supplemental Experimental Procedures.

Quantification of Endothelial Nets

Net formation capacity was determined by quantification of branching points per net and cell culture plate after IB4 (Vector) and DAPI staining.

Capillary Density

Capillary density was determined as the ratio of capillaries to cardiomyocytes in transversely sectioned LVs stained IB4 (Vector) and with wheat germ agglutinin (WGA, Vector) and Hoechst 33258, as described previously (Hilfiker-Kleiner et al., 2007).

Isolation of RNA and qRT-PCR

Total RNA isolation from adult murine heart, kidney, liver, CPCs, and NRCM and qRT-PCR (Brilliant SYBR Green Mastermix-Kit, Stratagene) performed with the Stratagene MX3005P multiplex QPCR System was described previously (Hilfiker-Kleiner et al., 2007). Primer sequences are provided in the Supplemental Experimental Procedures.

Generation of the CCR2 Antagonizing Cleavage Product

WT and CKO hearts were minced and resuspended in 70 μl DMEM per 25 mg of tissue supplemented with rCCL2 (250 ng) and/or PF-356231 (30 nM) over 6 hr at 37°C.

Luciferase Assay

Cloning of the putative CCL2-promoter in the luciferase reporter plasmid pGL4.12 is described in the Supplemental Information. NRCM were transiently transfected with 3 μg DNA/well of mouse CCL2 promoter-pGL4.12 luc construct or with pGL4.12 luc (Promega) using Lipofectamin 2000 (Invitrogen). 12 hr after transfection, cells were stimulated with EPO (1.2 U/ml), TNFα (10 ng/ml), and LPS (4 μg/ml). After 24 hr stimulation, cells were harvested and luciferase activity was determined by using dual-luciferase reporter assay system (Promega) according to manufacturer's protocol.

Immunoblotting

Immunoblots were performed according to standard procedures using SDS-PAGE (Hilfiker-Kleiner et al., 2004). The following antibodies were used: Actin (SIGMA), STAT3 (Cell Signaling), EPO (BD PharMingen; Santa Cruz Biotechnology), and CCL2 (Santa Cruz Biotechnology).

EPO ELISA

Concentrations of EPO in cardiomyocyte supernatants were measured using a commercial EPO enzyme-linked-immunosorbent assay according to the manufacturer's protocol (Quantikine, R&D Systems).

Statistical Analyses

Data are presented as mean ± SD. Differences between groups were analyzed by Student's t test or ANOVA followed by Bonferroni as appropriate. A two-tailed p value of < 0.05 was considered to indicate statistical significance.

ACCESSION NUMBERS

The microarray data are available in the Gene Expression Omnibus (GEO) database (http://www.ncbi.nlm.nih.gov/gds) under the accession number GSE30306.

SUPPLEMENTAL INFORMATION

Supplemental Information includes Supplemental Experimental Procedures, six figures, and two tables and can be found with this article online at doi:10.1016/j.stem.2011.07.001.

ACKNOWLEDGMENTS

We thank the cell sorting core facility and the core facility for laser microscopy of the Hannover Medical School (Braukmann-Wittenberg-Herz-Stiftung and DFG), Martina Kasten, Tibor Horvath, Silvia Gutzke, Sergej Erschow, Inga Sörensen, and Birgit Brandt for excellent technical assistance. This work was supported by the DFG (HI 842/3-2 and REBIRTH) and the Foundation Leducq.

Received: July 13, 2010
Revised: May 31, 2011
Accepted: July 5, 2011
Published: August 5, 2011

REFERENCES

Asaumi, Y., Kagaya, Y., Takeda, M., Yamaguchi, N., Tada, H., Ito, K., Ohta, J., Shiroto, T., Shirato, K., Minegishi, N., and Shimokawa, H. (2007). Protective role of endogenous erythropoietin system in nonhematopoietic cells against pressure overload-induced left ventricular dysfunction in mice. Circulation *115*, 2022–2032.

Benedito, R., Roca, C., Sörensen, I., Adams, S., Gossler, A., Fruttiger, M., and Adams, R.H. (2009). The notch ligands Dll4 and Jagged1 have opposing effects on angiogenesis. Cell *137*, 1124–1135.

Bergmann, M.W., Haufe, S., von Knobelsdorff-Brenkenhoff, F., Mehling, H., Wassmuth, R., Münch, I., Busjahn, A., Schulz-Menger, J., Jordan, J., Luft, F.C., and Dietz, R. (2011). A pilot study of chronic, low-dose epoetin-beta following percutaneous coronary intervention suggests safety, feasibility, and efficacy in patients with symptomatic ischaemic heart failure. Eur. J. Heart Fail. *13*, 560–568.

Chen, X., Chen, Y., Bi, Y., Fu, N., Shan, C., Wang, S., Aslam, S., Wang, P.W., and Xu, J. (2007). Preventive cardioprotection of erythropoietin against doxorubicin-induced cardiomyopathy. Cardiovasc. Drugs Ther. *21*, 367–374.

Contreras-Shannon, V., Ochoa, O., Reyes-Reyna, S.M., Sun, D., Michalek, J.E., Kuziel, W.A., McManus, L.M., and Shireman, P.K. (2007). Fat accumulation with altered inflammation and regeneration in skeletal muscle of CCR2-/- mice following ischemic injury. Am. J. Physiol. Cell Physiol. *292*, C953–C967.

Dean, R.A., Cox, J.H., Bellac, C.L., Doucet, A., Starr, A.E., and Overall, C.M. (2008). Macrophage-specific metalloelastase (MMP-12) truncates and inactivates ELR+ CXC chemokines and generates CCL2, -7, -8, and -13 antagonists: Potential role of the macrophage in terminating polymorphonuclear leukocyte influx. Blood *112*, 3455–3464.

Deng, J., Grande, F., and Neamati, N. (2007). Small molecule inhibitors of Stat3 signaling pathway. Curr. Cancer Drug Targets *7*, 91–107.

El Hasnaoui-Saadani, R., Pichon, A., Marchant, D., Olivier, P., Launay, T., Quidu, P., Beaudry, M., Duvallet, A., Richalet, J.P., and Favret, F. (2009). Cerebral adaptations to chronic anemia in a model of erythropoietin-deficient mice exposed to hypoxia. Am. J. Physiol. Regul. Integr. Comp. Physiol. *296*, R801–R811.

Ferreira, A.L., Matsubara, L.S., and Matsubara, B.B. (2008). Anthracycline-induced cardiotoxicity. Cardiovasc. Hematol. Agents Med. Chem. *6*, 278–281.

Gewirtz, D.A., Di, X., Walker, T.D., and Sawyer, S.T. (2006). Erythropoietin fails to interfere with the antiproliferative and cytotoxic effects of antitumor drugs. Clin. Cancer Res. *12*, 2232–2238.

Haghikia, A., Missol-Kolka, E., Tsikas, D., Venturini, L., Brundiers, S., Castoldi, M., Muckenthaler, M.U., Eder, M., Stapel, B., Thum, T., et al. (2010). STAT3-mediated regulation of miR-199a-5p links cardiomyocyte and endothelial cell function in the heart: A key role for ubiquitin-conjugation enzymes. Eur. Heart J. *32*, 1287–1297.

Hilfiker-Kleiner, D., Hilfiker, A., Fuchs, M., Kaminski, K., Schaefer, A., Schieffer, B., Hillmer, A., Schmiedl, A., Ding, Z., Podewski, E., et al. (2004). Signal transducer and activator of transcription 3 is required for myocardial capillary growth, control of interstitial matrix deposition, and heart protection from ischemic injury. Circ. Res. *95*, 187–195.

Hilfiker-Kleiner, D., Kaminski, K., Podewski, E., Bonda, T., Schaefer, A., Sliwa, K., Forster, O., Quint, A., Landmesser, U., Doerries, C., et al. (2007). A cathepsin D-cleaved 16 kDa form of prolactin mediates postpartum cardiomyopathy. Cell *128*, 589–600.

Hsieh, P.C., Segers, V.F., Davis, M.E., MacGillivray, C., Gannon, J., Molkentin, J.D., Robbins, J., and Lee, R.T. (2007). Evidence from a genetic fate-mapping study that stem cells refresh adult mammalian cardiomyocytes after injury. Nat. Med. *13*, 970–974.

Iwakura, T., Mohri, T., Hamatani, T., Obana, M., Yamashita, T., Maeda, M., Katakami, N., Kaneto, H., Oka, T., Komuro, I., et al. (2011). STAT3/Pim-1 signaling pathway plays a crucial role in endothelial differentiation of cardiac resident Sca-1+ cells both in vitro and in vivo. J. Mol. Cell. Cardiol. *51*, 207–214.

Jacoby, J.J., Kalinowski, A., Liu, M.G., Zhang, S.S., Gao, Q., Chai, G.X., Ji, L., Iwamoto, Y., Li, E., Schneider, M., et al. (2003). Cardiomyocyte-restricted knockout of STAT3 results in higher sensitivity to inflammation, cardiac fibrosis, and heart failure with advanced age. Proc. Natl. Acad. Sci. USA *100*, 12929–12934.

Kittleson, M.M., Minhas, K.M., Irizarry, R.A., Ye, S.Q., Edness, G., Breton, E., Conte, J.V., Tomaselli, G., Garcia, J.G.N., and Hare, J.M. (2005). Gene expression analysis of ischemic and nonischemic cardiomyopathy: shared and distinct genes in the development of heart failure. Physiol. Genomics *21*, 299–307.

Kunisada, K., Negoro, S., Tone, E., Funamoto, M., Osugi, T., Yamada, S., Okabe, M., Kishimoto, T., and Yamauchi-Takihara, K. (2000). Signal transducer and activator of transcription 3 in the heart transduces not only a hypertrophic signal but a protective signal against doxorubicin-induced cardiomyopathy. Proc. Natl. Acad. Sci. USA *97*, 315–319.

Lin, J.S., Chen, Y.S., Chiang, H.S., and Ma, M.C. (2008). Hypoxic preconditioning protects rat hearts against ischaemia-reperfusion injury: Role of erythropoietin on progenitor cell mobilization. J. Physiol. *586*, 5757–5769.

Madonna, R., Shelat, H., Xue, Q., Willerson, J.T., De Caterina, R., and Geng, Y.J. (2009). Erythropoietin protects myocardin-expressing cardiac stem cells against cytotoxicity of tumor necrosis factor-alpha. Exp. Cell Res. *315*, 2921–2928.

Miller, C.L., and Lai, B. (2005). Human and mouse hematopoietic colony-forming cell assays. Methods Mol. Biol. *290*, 71–89.

Mohri, T., Fujio, Y., Obana, M., Iwakura, T., Matsuda, K., Maeda, M., and Azuma, J. (2009). Signals through glycoprotein 130 regulate the endothelial differentiation of cardiac stem cells. Arterioscler. Thromb. Vasc. Biol. *29*, 754–760.

Najjar, S.S., Rao, S.V., Melloni, C., Raman, S.V., Povsic, T.J., Melton, L., Barsness, G.W., Prather, K., Heitner, J.F., Kilaru, R., et al; REVEAL Investigators. (2011). Intravenous erythropoietin in patients with ST-segment elevation myocardial infarction: REVEAL: A randomized controlled trial. JAMA *305*, 1863–1872.

Nakagami, H., Nakagawa, N., Takeya, Y., Kashiwagi, K., Ishida, C., Hayashi, S., Aoki, M., Matsumoto, K., Nakamura, T., Ogihara, T., and Morishita, R. (2006). Model of vasculogenesis from embryonic stem cells for vascular research and regenerative medicine. Hypertension *48*, 112–119.

Oh, H., Bradfute, S.B., Gallardo, T.D., Nakamura, T., Gaussin, V., Mishina, Y., Pocius, J., Michael, L.H., Behringer, R.R., Garry, D.J., et al. (2003). Cardiac progenitor cells from adult myocardium: Homing, differentiation, and fusion after infarction. Proc. Natl. Acad. Sci. USA *100*, 12313–12318.

Pittenger, M.F., and Martin, B.J. (2004). Mesenchymal stem cells and their potential as cardiac therapeutics. Circ. Res. *95*, 9–20.

Podewski, E.K., Hilfiker-Kleiner, D., Hilfiker, A., Morawietz, H., Lichtenberg, A., Wollert, K.C., and Drexler, H. (2003). Alterations in Janus kinase (JAK)-signal transducers and activators of transcription (STAT) signaling in patients with end-stage dilated cardiomyopathy. Circulation *107*, 798–802.

Salcedo, R., Ponce, M.L., Young, H.A., Wasserman, K., Ward, J.M., Kleinman, H.K., Oppenheim, J.J., and Murphy, W.J. (2000). Human endothelial cells express CCR2 and respond to MCP-1: Direct role of MCP-1 in angiogenesis and tumor progression. Blood *96*, 34–40.

Tada, H., Kagaya, Y., Takeda, M., Ohta, J., Asaumi, Y., Satoh, K., Ito, K., Karibe, A., Shirato, K., Minegishi, N., and Shimokawa, H. (2006). Endogenous erythropoietin system in non-hematopoietic lineage cells plays a protective role in myocardial ischemia/reperfusion. Cardiovasc. Res. *71*, 466–477.

Tammela, T., Zarkada, G., Wallgard, E., Murtomäki, A., Suchting, S., Wirzenius, M., Waltari, M., Hellström, M., Schomber, T., Peltonen, R., et al. (2008). Blocking VEGFR-3 suppresses angiogenic sprouting and vascular network formation. Nature *454*, 656–660.

Tamura, Y., Matsumura, K., Sano, M., Tabata, H., Kimura, K., Ieda, M., Arai, T., Ohno, Y., Kanazawa, H., Yuasa, S., et al. (2011). Neural crest-derived stem cells migrate and differentiate into cardiomyocytes after myocardial infarction. Arterioscler. Thromb. Vasc. Biol. *31*, 582–589.

Tarzami, S.T., Calderon, T.M., Deguzman, A., Lopez, L., Kitsis, R.N., and Berman, J.W. (2005). MCP-1/CCL2 protects cardiac myocytes from hypoxia-induced apoptosis by a G(alphai)-independent pathway. Biochem. Biophys. Res. Commun. *335*, 1008–1016.

Tepper, O.M., Galiano, R.D., Capla, J.M., Kalka, C., Gagne, P.J., Jacobowitz, G.R., Levine, J.P., and Gurtner, G.C. (2002). Human endothelial progenitor cells from type II diabetics exhibit impaired proliferation, adhesion, and incorporation into vascular structures. Circulation *106*, 2781–2786.

Torella, D., Rota, M., Nurzynska, D., Musso, E., Monsen, A., Shiraishi, I., Zias, E., Walsh, K., Rosenzweig, A., Sussman, M.A., et al. (2004). Cardiac stem cell and myocyte aging, heart failure, and insulin-like growth factor-1 overexpression. Circ. Res. *94*, 514–524.

Ueba, H., Brines, M., Yamin, M., Umemoto, T., Ako, J., Momomura, S., Cerami, A., and Kawakami, M. (2010). Cardioprotection by a nonerythropoietic, tissue-protective peptide mimicking the 3D structure of erythropoietin. Proc. Natl. Acad. Sci. USA *107*, 14357–14362.

Vogiatzi, G., Briasoulis, A., Tousoulis, D., Papageorgiou, N., and Stefanadis, C. (2010). Is there a role for erythropoietin in cardiovascular disease? Expert Opin. Biol. Ther. *10*, 251–264.

Zelarayán, L.C., Noack, C., Sekkali, B., Kmecova, J., Gehrke, C., Renger, A., Zafiriou, M.P., van der Nagel, R., Dietz, R., de Windt, L.J., et al. (2008). Beta-Catenin downregulation attenuates ischemic cardiac remodeling through enhanced resident precursor cell differentiation. Proc. Natl. Acad. Sci. USA *105*, 19762–19767.